Original Research Paper

JIC *Journal of Industrial Catalysis*
Vol. 1, No. 2, 2024, 66-71

TEMPO@$FeNi_3$/DFNS-Laccase Magnetic Nanocatalyst: Synthesis, Characterization, and Catalytic Reduction of 4-Nitrophenol in Wastewater

Zahra Dorostgou[1], Malihesadat Hosseiny [2*], Afsaneh Bahrami[3], Rahele Zhiani[2], Mahnaz Mohtashami[4]

1Department of Biochemistry, Ne.C., Islamic Azad University, Neyshabur, Iran
2Department of Chemistry, Ne.C., Islamic Azad University, Neyshabur, Iran.
3Clinical Research Development Unit, Imam Reza Hospital, Faculty of Medicine, Mashhad University of Medical Sciences, Mashhad, Iran
4Department of Microbiology, Ne.C., Islamic Azad University, Neyshabur, Iran
* malihesadat.hosseiny@iau.ac.ir

Received 19 August 2025; accepted 4 October 2025

Abstract

In this study, magnetic $FeNi_3$ nanoparticles with a dendritic fibrous nanosilica (DFNS) structure were synthesized via chemical precipitation. The nanoparticles were functionalized with TEMPO and immobilized laccase to obtain TEMPO-$FeNi_3$@DFNS-laccase nanocatalysts. Structural and surface modification were confirmed by FTIR, XRD, SEM, and TEM analyses. The nanocatalysts demonstrated excellent catalytic efficiency in reducing 4-nitrophenol to 4-aminophenol in water using $NaBH_4$ as the reducing agent, achieving 99% conversion within 120 seconds. Enzyme activity studies (with ABTS substrate) and tests on pH, temperature, and repeated use indicated high stability and recyclability, with 90% activity retained after five cycles and thermal stability up to 80°C. The magnetic properties allowed rapid separation and reuse. These findings highlight the crucial role of DFNS modification in enhancing catalytic performance and provide a green, efficient strategy for wastewater treatment.

Keywords: *Laccase, Alginate, Enzyme Immobilization, Microorganism, Catalyst, Nanoparticle*

1. Introduction

Water pollution has emerged as a serious global concern, threatening the entire biosphere and affecting the lives of countless individuals worldwide. Various diseases are caused by water contamination, and many people die each year from waterborne illnesses.

To date, numerous studies have reported the removal of nitro compounds from wastewater and environmental pollutants using nanoparticles [1–5]. Enzymes, as nanoscale biocatalysts, possess diverse and well-established capabilities. In the past, enzymes were primarily employed in industrial processes, particularly in detergent production. Currently, their applications have significantly expanded into novel areas such as pharmaceuticals, biosensing, biological pollutant removal, bioseparation, and biofuel cells [6].

However, free enzymes often exhibit limited stability against pH and temperature variations and are difficult to recover. Therefore, improving enzyme stability is of great importance [7]. The utilization of nanostructures for enzyme immobilization and stabilization not only enhances enzyme stability but also results in higher enzyme loading, increased catalytic activity, and improved ease of recovery.

Enzyme adsorption onto carriers may occur through different types of interactions. Enzymes with highly lipophilic surfaces form favorable binding with hydrophobic carriers. Van der Waals forces and entropic changes further support the immobilization of enzymes on carriers. Additionally, the sugar residues of glycosylated enzymes can stabilize adsorption through hydrogen bonding, while hydrophilic regions of enzymes readily interact with hydrophilic supports [8]. Depending on the pH and isoelectric point of the solution, enzyme surfaces may carry a charge, which can be predicted using modeling systems to determine charge distribution [9].

Compared to biological, physical, and chemical purification processes, enzymatic treatment offers several advantages. Among the enzymes capable of degrading phenolic compounds, peroxidase extracted from horseradish roots is one of the most widely studied [10]. Many microorganisms, including bacteria, fungi, and algae, possess the ability to degrade phenol. For instance, bacterial consortia of the *Pseudomonas* genus are

commonly used for the biological degradation of phenol and biomass production [11].

Laccases, due to their ability to oxidize a broad range of substrates, have been applied in multiple industrial sectors. Recently, the synthesis of nanoparticles with magnetic properties has gained significant attention. The use of stabilizers or surfactants helps maintain particle size and control morphology, thereby preventing undesirable aggregation [12].

Liposomes, as drug delivery carriers, have found expanded applications in nanomedicine. One of the benefits of encapsulating nanoparticles in liposomes is the prolonged circulation time in blood, the ability to carry a larger number of magnetic nanoparticle cores, and simultaneous delivery to target tissues, which significantly reduces dilution effects [13].

In 2011, Karimi and Farhang reported magnetic core–shell nanoparticles with high recyclability, supported with a TEMPO catalyst for alcohol oxidation. After use, the magnetic catalyst was easily separated and reused for consecutive reactions [14].

In the study by Mohammadi and colleagues, magnetic nanoparticles were synthesized through chemical co-precipitation and in situ coating. Following synthesis, the coated nanoparticles were applied for the removal of malachite green, and the effects of factors such as pH and temperature were investigated. The results revealed that higher removal efficiency was achieved with increasing pH and temperature [15]. Similarly, Mai and co-workers employed a modified two-step co-precipitation method followed by in situ coating. Their findings indicated nanoparticles with cores of 5–10 nm and hydrodynamic diameters ranging from 194 to 483 nm. These nanoparticles remained stable in terms of size and zeta potential for up to 12 months at 4 °C and pH 7 [16].

In another study, Chang and colleagues examined the effects of various parameters on the immobilization of laccase onto amine-modified magnetic iron nanoparticles. The optimal conditions for immobilization were found to be approximately 11 hours of reaction time, 25 °C, and pH 8 [17].

Roges and co-workers investigated the oxidative removal of para-methoxyphenyl (PMP), used as an amine-protecting group, employing laccase under mildly acidic conditions [18].

2- Experimental method

2-1- Materials and Methods

High-purity chemical reagents were purchased from Fluka and Merck. Field-emission scanning electron microscopy (FE-SEM) images were obtained using a HITACHI model S-4160 instrument. Fourier-transform infrared (FTIR) spectra were recorded with a Bruker VERTEX spectrometer. X-ray diffraction (XRD) data were collected on a Bruker D8 Advance diffractometer using Cu Kα radiation. The pore volume and diameter of the nanoparticles were determined by N_2 adsorption at –196 °C using an ASAP Micromeritics analyzer. Additional pore size analyses were performed using different instruments. For stirring operations, an IKA magnetic stirrer with heating plate (UK) was employed. A laboratory oven (model UF119, Memmert, Germany), an electronic balance (model K0012), and a centrifuge (model 48 MF CENTRIC, Domel) were also utilized in this study.

2-2- Synthesis of $FeNi_3$ MNPs

The synthesis of $FeNi_3$ magnetic nanoparticles (MNPs) involved dissolving 0.01 mol $FeCl_2{\cdot}4H_2O$ and 0.03 mol $NiCl_2{\cdot}6H_2O$ in 300 mL of deionized water, followed by the addition of 1.0 g polyethylene glycol (PEG, MW 6000). To adjust the pH to the range of $12 \leq pH \leq 13$, sodium hydroxide (NaOH) was introduced into the solution. Subsequently, hydrazine hydrate ($N_2H_4{\cdot}H_2O$, 80%) in varying amounts was added to the suspension. The mixture was stirred continuously at room temperature for 24 hours, while the pH was maintained within $12 \leq pH \leq 13$ by periodic addition of NaOH. After the reaction, the resulting solid phase was filtered, yielding black $FeNi_3$ MNPs, which were washed several times with deionized water [19].

“This synthetic route yields $FeNi_3$-DFNS nanoparticles used as the main nanocatalyst in this study. The protocol in Section 2.8 was used only to synthesize Alg-$FeNi_3$ as a comparative sample.

2-3- Synthesis of $FeNi_3/SiO_2$ MNPs

An aqueous solution containing 80 mL ethanol, 20 mL deionized water, and 2.0 mL of 28% concentrated aqueous ammonia ($NH_3{\cdot}H_2O$) was prepared. Subsequently, 0.02 mol $FeNi_3$ MNPs were dispersed in the mixture, followed by the addition of 0.20 g tetraethyl orthosilicate (TEOS). The resulting suspension was stirred vigorously for 24 hours. The solid phase obtained was then filtered and washed several times.

2-4- Synthesis of $FeNi_3$/DFNS MNPs

Solution A was prepared by adding 30 mL of an aqueous solution containing 0.3 g urea and 0.25 g $FeNi_3/SiO_2$, followed by sonication in an ultrasonic bath for 1 hour. Solution B was prepared by dissolving 0.5 g cetylpyridinium bromide (CPB) in 0.75 mL n-pentanol and 30 mL cyclohexane. Solutions A and B were then mixed at room temperature, and 1.25 g tetraethyl orthosilicate (TEOS) was added dropwise. The mixture was stirred continuously at room temperature for 1 hour and subsequently heated at 120 °C for 5 hours to initiate the reaction. After cooling to room temperature, the core–shell $FeNi_3$/DFNS microspheres were separated using a strong magnetic field. The solid phase was washed several times with water and acetone, dried in an oven at 40 °C, and finally calcined at 550 °C for 5 hours.

2-5- Synthesis of $FeNi_3$/DFNS/GMSI MNPs

A total of 200 mg $FeNi_3$/DFNS was dispersed in 20 mL THF, followed by the addition of 20 mmol NaH.

Subsequently, 22 mmol of (3-glycidyloxypropyl)trimethoxysilane was added to the mixture at room temperature, and the reaction was stirred at 50 °C for 16 hours. The resulting mixture was filtered and washed with ethanol and deionized water. The filtered solid was then dried under vacuum at 50 °C for 3 hours [19].

2-6- TEMPO@$FeNi_3$/DFNS-Laccase MNPs

For the activation of $FeNi_3$/DFNS, 100 mg of glycidyloxypropyl was employed. This activated material was then added to a mixture containing 10 mL acetate buffer (0.1 mM, pH 4.5), laccase, and 4-hydroxy-TEMPO. The mixture was stirred for several hours at 120 rpm. The resulting nanoparticles, containing immobilized laccase and TEMPO, were filtered and washed several times with acetate buffer. The filtered nanoparticles were stored at 4 °C for preservation

"This synthetic route yields $FeNi_3$-DFNS nanoparticles used as the main nanocatalyst in this study. The protocol in Section 2.8 was used only to synthesize Alg-$FeNi_3$ as a comparative sample.

2-7- Reduction of Nitro Compounds

"Reduction of nitro compounds was carried out using $NaBH_4$ as the primary reducing agent."
A suspension of 1.5 mmol $NaBH_4$ in 5 mL H_2O was added to the nitro compound (1 mmol) in the presence of 15 mg TEMPO@$FeNi_3$/DFNS-laccase in aqueous media at 50 °C, and the mixture was stirred. The progress of the reaction was monitored by thin-layer chromatography (TLC). Upon completion, the catalyst was removed and washed with ethanol. The reaction mixture was extracted with ethyl acetate and dried over Na_2SO_4. The product was purified by column chromatography using hexane–ethyl acetate as the eluent in varying concentrations to obtain the pure compound.

2-8- Synthesis and Coating of $FeNi_3$ Magnetic Nanoparticles by Co-precipitation
"For comparative studies, Alginate-coated FeNi3 nanoparticles were also prepared as described below. All main catalytic and structural analyses were, however, carried out using the DFNS-based nanocatalyst."
Initially, 30 mL of ammonium hydroxide solution was mixed with 20 mL of deionized water in a beaker to prepare an alkaline solution. In a separate beaker, 4.68 g of $NiCl_2 \cdot 6H_2O$ and 1.27 g of $FeCl_2 \cdot 4H_2O$ were dissolved in 5 mL of deionized water, after which 2 mL of 2% (w/v) sodium alginate solution was added. The mixture was stirred at room temperature using a magnetic stirrer for 60 minutes and was then transferred into a three-necked flask.

At this stage, the alkaline solution was added dropwise under a nitrogen atmosphere at 60 °C while the three-necked flask was vigorously stirred. The reaction was maintained under the same conditions for an additional 30 minutes after the complete addition of the alkaline solution. The resulting black precipitate was separated using a strong magnet and was washed three times with deionized water to remove impurities and unbound alginate. To enhance separation efficiency, the nanoparticle suspension was subjected to ultrasonic treatment for 5 minutes before each washing step. Finally, the Alg-$FeNi_3$ nanoparticles were dried in a vacuum oven at 80 °C for 21 hours to obtain the final product. For control experiments, Alg-$FeNi_3$ nanoparticles were synthesized according to this separate procedure."

2-9- Immobilization of Enzyme on Synthesized Nanoparticles
A total of 0.3 g of coated nanoparticles **was mixed** with 3 mg HRP in 20 mL of buffer at pH 8. After the addition of 1 mL of 52% glutaraldehyde, the mixture **was stirred** at 25 °C and 200 rpm for 21 hours. The resulting product **was collected** using a magnet and sequentially **washed** with phosphate buffer and deionized water. The immobilized enzymes **were stored** in water at 4 °C.

2-10- Evaluation of Activity and Stability of Immobilized Peroxidase

In the enzyme immobilization process, the primary goal is to achieve stability of enzymatic activity after repeated use and under various pH and temperature conditions. Therefore, evaluating the performance of the immobilized enzyme is of critical importance.

2-11- Evaluation of Immobilized Enzyme Activity under Temperature, pH, and Time Variations
To assess the changes in activity of the immobilized enzyme relative to the free enzyme, measurements were conducted under various pH and temperature conditions in two stages. In the first stage, temperature was varied from 20 to 80 °C at a constant pH of 8. In the second stage, pH was varied from 4 to 10 at a constant temperature of 37 °C.
To examine the long-term stability of the immobilized enzyme, the samples were stored in deionized water at 4 °C for 12 days. During this period, the activity of both free and immobilized enzymes was measured every three days according to the described method.

3- Results

3-1- Measurement of Free and Immobilized Laccase Activity on Functionalized Magnetic Supports

The activity of free and immobilized laccase was measured using ABTS (5 mM) as the substrate in 5 mM sodium acetate buffer at pH 5 and 25 °C. The enzymatic

activity was determined based on the increase in absorbance at 420 nm, corresponding to the formation of the oxidized ABTS product (Figure 1).

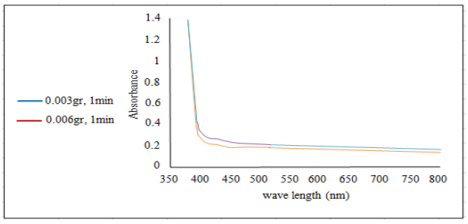

Figure 1 – Measurement of laccase activity using ABTS in sodium acetate buffer

The molar absorptivity for ABTS oxidation at 420 nm is 36,104 $M^{-1} \cdot cm^{-1}$.

3-2- Determination of Kinetic Parameters of Laccase and Immobilized Laccase on Functionalized Magnetic Supports

The initial reaction rates were measured at various ABTS concentrations (0.3–10 mM) in 100 mM sodium phosphate buffer (pH 5) at 25 °C.

3-3- Effect of Temperature and pH on Free and Immobilized Laccase Activity

To evaluate the resistance of free and immobilized laccase to pH variations, their activities were measured in different buffers ranging from pH 3 to 8 at 4 °C for 5 hours. The relative activity was calculated as the activity obtained at a given pH relative to the maximum activity (Figure 2).

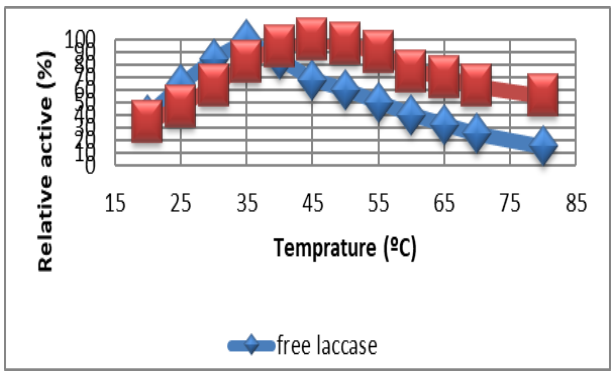

Figure 2 – Effect of temperature on the activity of free and immobilized laccase

3-4- Thermal Stability

The thermal stability of free and immobilized laccase was evaluated over a temperature range of 15–85 °C in 100 mM sodium phosphate buffer (pH 6) for 2 hours in an incubator. The enzymatic activity was measured at regular intervals using ABTS (Figure 3).

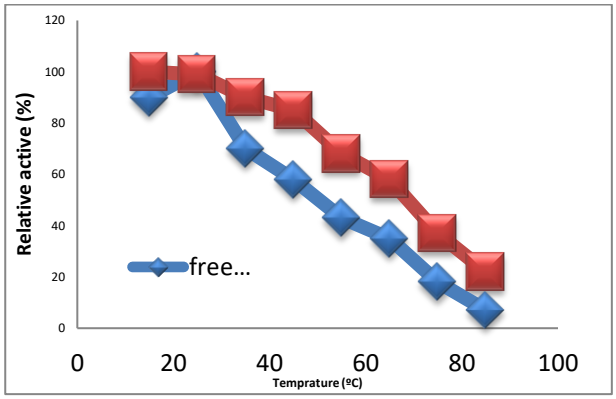

Figure 3 – Evaluation of thermal stability

3-5- TEM and FE-SEM Analysis of TEMPO@$FeNi_3$/DFNS-Laccase MNPs

TEM and FE-SEM images reveal spherical solids composed of fibrous structures. In Figure 4(a), $FeNi_3$/DFNS is observed to have a core consisting of $FeNi_3$ particles with a non-porous silica layer. A magnetic material and fibrous silica shell of magnetic $FeNi_3$/DFNS with a filamentous structure were also observed. TEM and FE-SEM images further indicate that no morphological changes occurred upon modification of $FeNi_3$/DFNS.

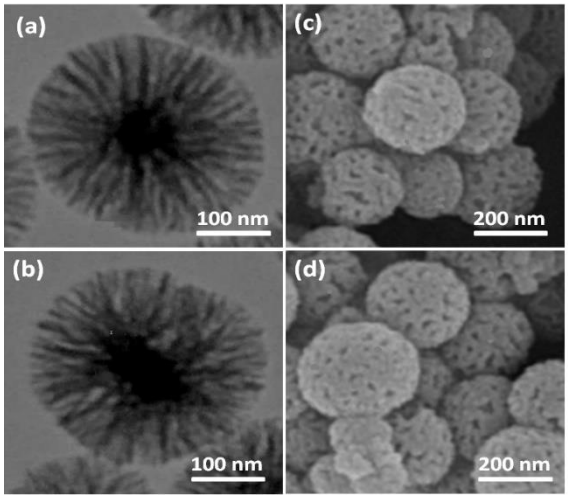

Figure 4 – TEM images of $FeNi_3$/DFNS MNPs (a) and TEMPO@$FeNi_3$/DFNS-laccase MNPs (b); FE-SEM images of $FeNi_3$/DFNS MNPs (c) and TEMPO@$FeNi_3$/DFNS-laccase MNPs (d)

3-6- XRD Analysis of TEMPO@$FeNi_3$/DFNS-Laccase MNPs

Figure 5 shows prominent diffraction peaks at 111, 200, and 220 for all samples. The obtained XRD patterns

match the reported standard $FeNi_3$ pattern in the JCPDS card (No. 19-0629), as shown in Figure 5(b). In Figure 5(a), a broad amorphous peak is observed, corresponding to the amorphous silica in the $FeNi_3$/DFNS core nanoparticles. The XRD pattern presented in Figure 5(c) for TEMPO@$FeNi_3$/DFNS-laccase MNPs appears normal and shows no noticeable changes.

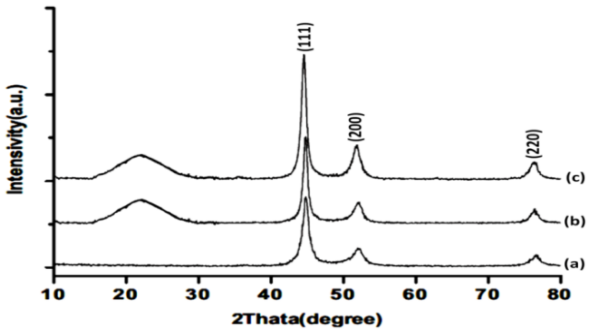

Figure 5 – XRD patterns of (a) $FeNi_3$, (b) $FeNi_3$/DFNS, and (c) TEMPO@$FeNi_3$/DFNS-laccase MNPs

3-7- FT-IR Analysis of TEMPO@$FeNi_3$/DFNS-Laccase MNPs

FTIR analysis revealed the presence of silanol, hydroxyl, and phosphate groups in $FeNi_3$/DFNS nanoparticles, with broad absorption bands at 1089 and 3654 cm^{-1}, respectively. The symmetric stretching and bending of Si–O–Si, observed at 799 and 467 cm^{-1}, indicate successful attachment of GMSI onto the DFNS surface. The bands around 1091, 793, and 462 cm^{-1} were exhibited by the GMSI–$FeNi_3$/DFNS composite. Stretching vibrations of OH and NH groups are evidenced by a strong and broad absorption band in the range of 3000–3550 cm^{-1} (Figure 6).

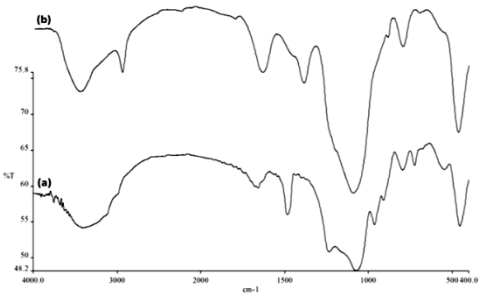

Figure 6 – FTIR spectra of (a) DFNS NPs and (b) GMSI–DFNS NPs

3-8- Evaluation of Catalytic Performance of TEMPO@$FeNi_3$/DFNS-Laccase MNPs

The catalytic activity of TEMPO@$FeNi_3$/DFNS-laccase MNPs was assessed via the reduction of 4-nitrophenol (4-NP) to 4-aminophenol (4-AP) in the presence of $NaBH_4$. The reaction progress was monitored using UV–Vis spectroscopy by tracking the time-dependent changes during the reduction of 4-NP to 4-AP. As shown in Figure 7(a), the 4-NP solution exhibits a prominent absorption peak at 400 nm, which corresponds to a noticeable color change from red to yellow.

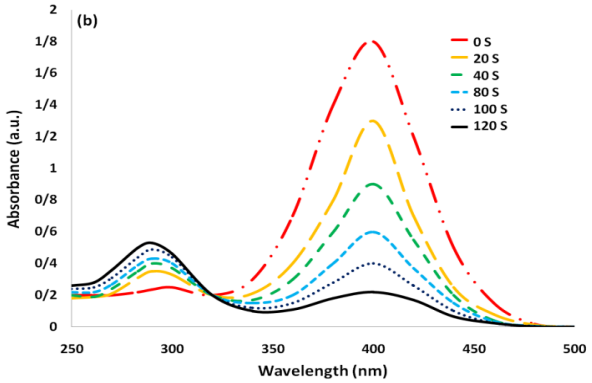

Figure 7 – UV–Vis spectra of (a) 4-NP before and after the addition of $NaBH_4$ solution, and (b) successive reduction of 4-NP to 4-AP

Using 15 mg of TEMPO@$FeNi_3$/DFNS-laccase MNPs in the system resulted in a decrease in the intensity of the 4-NP peak at 400 nm, accompanied by a simultaneous increase in the 4-AP peak at 300 nm. The reaction proceeded rapidly, achieving approximately 99% conversion within about 120 seconds (Figure 7(b)).

4-Conclusion

In this study, iron magnetic nanoparticles coated with laccase and alginate, with average sizes of 8.5 nm and 11 nm respectively, were successfully synthesized using the co-precipitation method. The TEMPO@$FeNi_3$/DFNS-laccase nanocatalyst was also successfully prepared and characterized. This nanocatalyst exhibited excellent catalytic performance in the reduction of aromatic nitro compounds under aqueous conditions, achieving 99% conversion within 120 seconds. Increasing the catalyst dosage beyond 15 mg resulted in minimal improvement, indicating active site saturation. The nanocatalyst demonstrated high thermal stability up to 80°C and retained 90% of its initial activity after five consecutive cycles. Furthermore, its magnetic properties allowed rapid separation and efficient reuse. These results highlight the potential of TEMPO@$FeNi_3$/DFNS-laccase

MNPs as a green and effective catalyst for environmental pollutant removal.

References

[1]B. Hamza, N. Zain, et al., Sustainable Chemistry and Pharmacy, 43 (2025) 101867.
[2] J. Kanwal, S. Musaddiq, et al., RSC Adv., 15(21) (2025) 16607-16621.
[3] L. Shoomaila, I. Muhammad, N. Muhammad, F. Marcelo, Adv. Chem. Pollut. Environ. Manag. Prot., 12 (2025) 665-687.
[4] M. Kazemnejadi, Results Chem., 13 (2025) 101995.
[5] B. El Allaoui, H. Chakhtouna, et al., Int. J. Biol. Macromol., 273(2) (2024) 133078.
[6] C. Lagrost, L. Preda, E. Volanschi, P. Hapiot, J. Electroanal. Chem., 585 (2005) 1-7.
[7] F. Cardenas-Lizana, S. Gomez-Quero, M. A. Keane, Catal. Commun., 9 (2008) 475-481.
[8]S. Pahujani, S. S. Kanwar, G. Chauhan, R. Gupta, Bioresour. Technol., 99 (2008) 2566-2570.
[9]V. Minovska, E. Winkelhausen, S. Kuzmanova, J. Serb. Chem. Soc., 70 (2005) 609-624.
[10]F. Vipulanandan, C. Li, K.K. Mohanty, Colloids Surfaces A., 223 (2003) 103-112.
[11] J. Durand, Eur. J. Inorg. Chem., 23 (2008) 3577-3586.
[12] M. Bowker, Surf. Sci., 603 (2005) 2359-2362.
[13] V.P. Torchilin, Nat. Rev. Drug Discov., 4 (2005) 145-160.
[14] B. Karimi, E. Farhang, J. Chem. Eur., 17 (2011) 6056.
[15] A. Mohammadi, H. Daemi, M. Barikani, Int. J. Biol. Macromol., 75 (2015) 447-445.
[16] H.-l. Ma, X.-r. Qi, Y. Maitani, T. Nagai, Int. J. Pharm., 329 (2007) 177-186.
[17]Q. Chang, H. Tang, Molecules, 23 (2018) 15768-15782.
[18] L. Cabrera, S. Gutierrez, N. Menendez, M.P. Morales, P. Herrasti, Electrochem. Acta., 53 (2008) 3436-3441.
[19] L. Fan, J. Wang, X. Zhang, S.M. Sadeghzadeh, R. Zhiani, M. Shahroudi, F. Amarloo, Catal. Lett., 149 (2019) 3465-3475.